Sensitivity of the selective oxidation of methane over Fe/ZSM-5 zeolites in a micro fixed-bed reactor for the catalyst preparation method

Sensitivity of the Selective Oxidation of Methane over Fe/ZSM-5 zeolites in a Micro Fixed-Bed Reactor for the Catalyst Preparation Method

Hualiang Zuo[a,*], Qi Xin[b], Vera Meynen[b], and Elias Klemm[a,*]

[a] Hualiang Zuo, Prof. Dr.-Ing. Elias Klemm, University of Stuttgart, Institute of Chemical Technology, Faculty of Chemistry, Pfaffenwaldring 55, 70569 Stuttgart, Germany; [b] Qi Xin, Prof. Dr. Vera Meynen, University of Antwerp, Laboratory of Adsorption and Catalysis, Department of Chemistry, Universiteitsplein 1, B-2610 Wilrijk, Belgium.

* Corresponding authors. E-mail addresses: hualiang.zuo@itc.uni-stuttgart.de (H.Zuo), elias.klemm@itc.uni-stuttgart.de (E.Klemm).

Graphical abstract

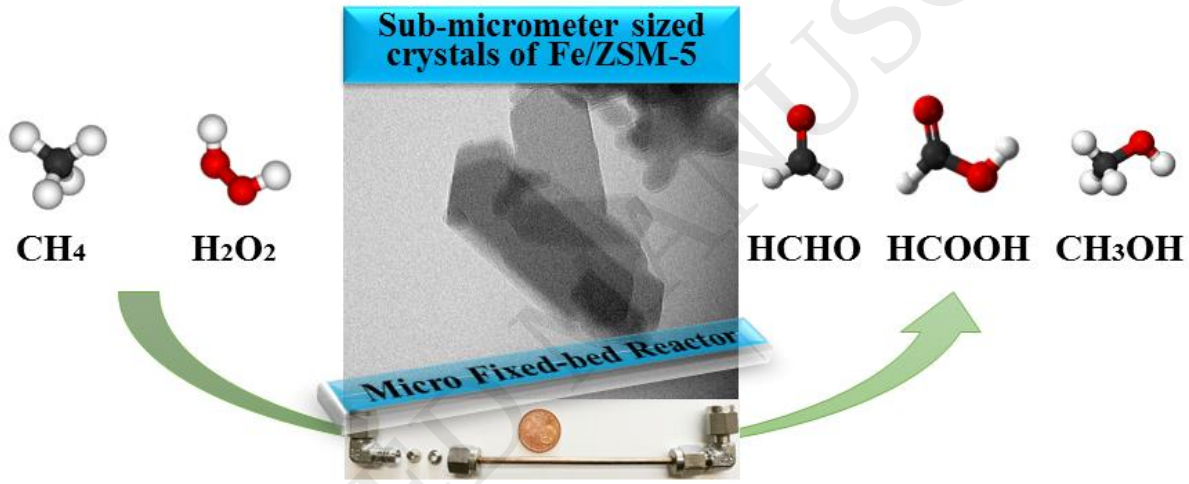

Highlights:

1, Turnover frequencies and volumetric productivities significantly increase by the use of sub-micrometer sized crystals of Fe/ZSM-5 and a micro reactor.

2, The activities of post-synthesis loaded Fe/ZSM-5 zeolites do not depend on the preparation method.

3, Brønsted acidity can't activate methane under given conditions.

4, Fe/silicalite-1 with the same Fe loading as Fe/ZSM-5 does not show any activity.

5, The over-oxidation level decreases on Fe/ZSM-5 by using Fe(II) precursors instead of Fe(III) precursors.

Abstract:

Selective oxidation of methane in a micro fixed-bed reactor by using aqueous H_2O_2 solution as oxidant was studied. Sub-micrometer sized crystals of HZSM-5 and silicalite-1 with Fe contents below 10 ppm were synthesized. Different methods were used to introduce iron to produce Fe/ZSM-5 zeolites with similar but defined Fe contents. Commercial ZSM-5 with trace amount (175 ppm) of Fe impurity showed considerable methane conversion while over the own nearly Fe-free HZSM-5 no conversion could be measured. Fe/ZSM-5 catalysts prepared by different methods starting from the own nearly Fe-free HZSM-5 showed similar methane conversions and catalysts based on Fe(II) as the precursor exhibited a better performance with regard to retarding over-oxidation. The productivities of oxygenates were enhanced more than two orders of magnitude while at the same time obtaining high turnover frequencies (TOFs) of 303 h^{-1}. A methane conversion as high as 23.5 % together with oxygenates selectivity of 90.1 % was reached. In contrast to Fe/ZSM-5, Fe/silicalite-1, prepared from Fe-free silicalite-1 by activation via the same post-synthetic preparation methods that were also used to prepare Fe/ZSM-5 and having similar Fe contents, never led to an active catalyst.

Keywords: *Methane selective oxidation, Hydrogen Peroxide, Fe/ZSM-5, Fe/silicalite-1, Micro reactor*

1 Introduction

In current chemical industry, selective oxidation reactions play an important role for the producing of key intermediates such as epoxides, aldehydes, alcohols, organic acids and ketones [1]. Among the selective oxidation of hydrocarbons, the selective oxidation of methane to oxygenates is a key challenge. This is because methane is a highly symmetric and extremely stable molecule, which doesn't exhibit any dipolar instant or features that would permit for directing chemical reactions [2]. In methane, the carbon-hydrogen bond owns a quite high bond energy (104 kcal•mol^{-1} per C-H bond), which usually requires high temperature in gas phase or other harsh conditions for activation and in most case inevitably causes radical reactions with inherent low selectivity [3, 4]. Due to these reasons, nowadays a widely established path for the utilization of methane contains firstly an endothermic steam reforming step to obtain syngas (H_2 + CO) and

secondly a Fischer-Tropsch or methanol synthesis process to produce organic oxygenates. It is obvious that this route is energy-intensive and cost-intensive, which become profitable only at very large scales [5, 6]. Thereby, alternative paths such as the directly selective oxidation of methane to produce chemicals and fuels are of significant interests, especially for decentralized smaller plants and received intensive investigations [7-15].

Nature often bears magical power. In nature, methanotrophic bacteria can selectively oxidize methane to methanol via a mild and controlled oxidation process using methane monooxygenase enzymes (MMOs) [16, 17]. Di-iron sites in the soluble MMO and di-copper sites in the particulate MMO are attributed to be the active species [18]. These binuclear sites create bridged oxidizing species that are powerful enough to activate the carbon-hydrogen in methane [10]. ZSM-5, a kind of pentasil zeolite, which has a microporous structure, can stabilize binuclear sites similar to those appeared in MMOs. It is reported that based on ZSM-5, binuclear Fe species could be obtained via different kinds of preparation methods such as solid state ion exchange (SSIE), liquid ion exchange (LIE) and chemical vapor deposition (CVD) [19-23]. However, the sensitivity of these different post-synthesis preparation methods to the selective oxidation of methane is still not clear. Recently, G. J. Hutchings and co-workers selectively oxidized methane to methanol by using aqueous H_2O_2 solution as oxidant in a batch reactor with Cu promoted Fe/ZSM-5 as catalysts [24]. Binuclear Fe species were assumed to be the active sites and TOF as high as 70 h^{-1} with low volumetric productivity regarding methanol was received. However, over the same catalyst, the value of TOF significantly dropped compared to one obtained in the batch reactor when the reaction was switched to continuous operation [14]. This make them propose that serious mass transport limitations arise in the continuous operation during the reaction [14]. Over Cu-Fe/ZSM-5 catalysts and based on similar reaction conditions with G. J. Hutchings's work, K. Hellgardt and co-workers [25] investigated the effect of different Si/Al ratios for the selective oxidation of methane to methanol. They proposed a significant effect on catalytic activity is because of the increasing of Brønsted acid sites in ZSM-5. However, trace impurity of Fe was detected in the parent ZSM-5 samples they used. As Fe is the active component for the activity, it is important to obtain iron free ZSM-5 before loading them with iron.

In this work, iron free ZSM-5 and silicalite-1 were synthesized. To compare the effect of different Fe loading methods on the activity and selectivity in the oxidation of methane with

aqueous hydrogen peroxide, SSIE, LIE and molecular designed dispersion (MDD) methods were used to prepare Fe/ZSM-5 catalysts with similar Fe contents. In order to obtain highly dispersed metal oxide layers on support materials without the generating of large oxide crystals, MDD method was developed [26-28]. The mainly principle of MDD is that acetylacetone metal complexes can react with the hydroxyl groups on the surface of the support materials and via a mild calcination process, metal oxide species could be highly dispersed on the supports [26-28]. In order to ensure a determined flow regime and improve external mass transport, a micro reactor was used. Based on our former study [29], it was shown that 100 °C is an optimized reaction temperature under given conditions, as higher temperatures lead to higher level over-oxidation of methane while lower temperatures such as 70 °C lead to a poorer productivity or even no reaction when the reaction temperature is 50 °C. A relative low concentration of aqueous H_2O_2 solution (0.12 M) with a relative large flow rate (1.5 ml•min^{-1}) was preferable for methane selective oxidation, since it decreases the over-oxidation level under given conditions [29]. So these conditions were used in this work where the focus is put on the sensitivity of the catalytic conversion and selectivity for the catalyst preparation method and zeolite support. The physicochemical properties of the catalysts were characterized by X-ray diffraction (XRD), inductively coupled plasma-optical emission spectrometry (ICP-OES), N_2 sorption, H_2-temperature-programmed reduction (H_2-TPR), NH_3-temperature-programmed desorption (NH_3-TPD), Transmission electron microscopy (TEM) and Ultraviolet-visible diffuse reflection spectroscopy (UV-Vis-DR) techniques.

2 Experimental

2.1 Materials and catalyst preparation

Commercial ZSM-5 (Si/Al=17) was obtained from Zeolyst in the ammonium form and was calcined at 550 °C for 3 hours to obtain the H-form (denoted as ZSM-5-C). Sub-micrometer sized crystals of HZSM-5 was synthesized according to R. Van Grieken et al. [30]. Aluminum isopropoxide (AIP, trace metals basis, Sigma-Aldrich) and tetraethyl orthosilicate (TEOS, trace metals basis, Sigma-Aldrich) were used as the aluminum and silica source. Tetrapropylammonium hydroxide aqueous solution (TPAOH, 40 wt. %, Alfa Aesar) with traces of Na was used as the template. Typically, 0.17 g of AIP was added to 4.87 g of 20 wt. % aqueous solution of TPAOH (diluted from 40 wt. % with double distilled water). The mixture was stirred at 0 °C for 2 hours.

Then 5.20 g of TEOS was added to the mixture drop by drop during stirring. A molar composition of $1Al_2O_3$:$60SiO_2$:21.4TPAOH:$650H_2O$ of the synthesis mixture is obtained. This mixture was stirred at room temperature for 44 hours and then was heated at 80 °C for 1.5 hours to remove alcohols and reduce the water content. Finally, the concentrated solution was crystallized at 170 °C for 4 days in a Teflon-lined stainless steel autoclave. The obtained materials were then washed with double distilled water, separated by a centrifuge and dried at 110 °C overnight in ambient air.

According to the recipe from A.E. Persson et al. [31] with modifications, silicalite-1 was synthesized. 22.39 mL of TEOS was firstly mixed with 26.81 mL of aqueous TPAOH (1.0 mol/L, Sigma-Aldrich) solution. After being stirred for 5 hours at room temperature, the homogenized gel was crystallized at 170 °C for 3 days in a Teflon-lined stainless steel autoclave. The as-synthesized materials were later washed with double distilled water, separated by a centrifuge and dried at 100 °C overnight in ambient air.

The dried ZSM-5 and silicalite-1 samples were ground in a pestle and mortar to powders and calcined at 550 °C (8 hours, 1 °C•min^{-1}) in flow of nitrogen (5 hours) and air (3 hours) to get template free samples (denoted as ZSM-5-S and Si-1, respectively).

The Fe loaded catalysts were prepared through various methods and different Fe precursor were used. The SSIE samples were prepared according to W. Grünert and co-workers [19]. A certain amount of $FeCl_3$ (trace metals basis, Sigma-Aldrich) was mixed with 2.0 g of ZSM-5-S followed by grinding in a pestle and mortar for 30 minutes. Under flowing N_2, the mixture was firstly heated to 150 °C (2 °C•min^{-1}) and then the temperature was increased to 300 °C (5 °C•min^{-1}) and hold for 1 hour. After cooling down, the sample was washed and dried at 100 °C overnight. Finally, the sample was calcined at 550 °C (1 °C•min^{-1}) for 3 hours in flow of air. These catalysts are denoted as Fe(III)/ZSM-5 SSIE. For comparison, Si-1 was also used as the support and denoted as Fe(III)/Si-1 SSIE.

The MDD catalysts were prepared as follows. The support was firstly dried at 200 °C in air for 6 hours prior to the synthesis. Then, in a dry air flushed glove box, 1.0 g of the dried powder was stirred in 30 mL anhydrous chloroform solution ($CHCl_3$, ≥99%, Sigma Aldrich) that contains 0.0316 g iron (III) acetylacetonate ($Fe(acac)_3$, 99%, Acros) or 0.023g iron (II) acetylacetonate ($Fe(acac)_2$, 99%, Chemos), to reach an ultimate Fe loading of 0.5 wt.%. The obtained mixture was stirred for 48 hours at ambient temperature and then was washed and filtrated 3 times with 10 mL

of chloroform. Afterwards, the samples were dried at 60 °C overnight in ambient air. At the end, the dried samples were calcined at 450 °C (6 hours, 1 °C•min^{-1}) in ambient air. These catalyst are denoted as Fe(III)/ZSM-5 MDD, Fe(II)/ZSM-5 MDD and Fe(III)/Si-1 MDD. The Roman numerals in the brackets indicate the valence of iron in the original Fe precursors (not in the final catalysts, since calcination is expected to give Fe(III)).

According to the method of A. Shishkin et al. [32], a LIE sample was prepared. 2.0 g of ZSM-5-S was added to 100 ml $FeCl_2$ (trace metals basis, Sigma-Aldrich) aqueous solution (0.045 mol/L) followed by stirring for 2 days at room temperature. The obtained sample was then washed with double distilled water until the rinsing solution did not contain Cl^{-1}, which was examined by the reaction of $AgNO_3$ with the rinsing solution. Then the received powder was dried at 110 °C overnight in ambient air and calcined at 450 °C for 3 hours in air (denoted as Fe(II)/ZSM-5 LIE).

2.2 Catalysts characterization

XRD patterns of the samples were obtained from a BrukerD8 Advance diffractometer (35 kV, 40 mA) with a Cu K_α (λ = 0.154 nm) radiation with a step size of 0.016 and a step time of 0.2 s.

Specific apparent surface area and micro pore volume were determined via N_2 isothermal sorption behavior at -196 °C employing a Quantachrome Autosorb IIIb device. The samples were degased at 350 °C for 16 hours in high vacuum before sorption.

Chemical Analysis was carried out using an ICP-OES spectrometer (Vista-MPX CCD) from Varian. Silicon, aluminum, and iron were determined by ICP-OES. Approximate 50 mg of the sample was firstly dissolved in 3 mL of diluted hydrofluoric acid (10 wt. % HF) and 6 mL of nitrohydrochloric acid (aqua regia). Then, this mixture was diluted to a final volume of 250 mL using doubly distilled water. After it, the diluted solution was analyzed.

UV-Vis-DR measurements of the catalysts were performed on a Nicolet Evolution 500 spectrophotometer in the range of 200-800 nm (scan speed of 120 nm•min^{-1}). The samples were diluted with KBr to a content of 2 wt. %. An average of three measuring cycles was taken for each sample.

TEM images were taken with an FEI TECNAI G^2. Before depositing of the sample on copper grids, the powder of the sample were suspended in acetone using an ultrasonic bath. The remaining

acetone was evaporated at ambient condition overnight. The applied voltage was 200 kV and the camera was a TVIPS TEMCAM F224HD.

H_2-TPR measurements were carried out on an Autosorb iQ (Quantachrome) instrument equipped with a thermal conductivity detector (TCD). The sample (formed particle sizes range from 200 μm to 315 μm) were firstly packed into a U-type quartz reactor. Then it was pre-treated in a He stream at 300 °C for 1 hour followed by cooling to 50 °C. After that, the reactor was heated (10 °C• min^{-1}) in a 10 vol. % of H_2 in N_2 gas flow (flow rate: 30 mL• min^{-1}) to 900 °C and was maintained at 900 °C for 30 min. The H_2 consumption was calibrated by performing H_2-TPR measurements of a known amount of CuO loaded on an inert support. NH_3-TPD measurements were performed on the same instrument. 75 mg of catalyst was firstly packed into the reactor. Then it was pre-treated in a N_2 flow (30 mL• min^{-1}) at 450 °C for 0.5 hour, followed by cooling to 120 °C for adsorbing ammonia until the saturated state was reached. After that, a flow of helium was purged for 1.5 hour at the same temperature to get rid of the physically adsorbed ammonia. Finally, the temperature was increased from 120 to 600 °C (10 °C• min^{-1}) and the NH_3-TPD profile was recorded.

2.3 Catalytic tests

The selective oxidation of methane was performed in a micro fixed-bed reactor. A flow-sheet of the experimental set-up is shown in Fig. S1. Detailed description of the set-up can be found in our former work [29]. Fig. S2 and Fig. S3 show the micro reactor and the plug flow found from the transparent pipe that installed before the reactor. The flow rate of the gas phase after the pressure controller was measured by a MilliGascounter (MGC-1 V3.4 PMMA, Ritter). H_2O_2 was quantified by the titration with acidified $Ce(SO_4)_2$ solution, using a Ferroin indicator.

The powders of catalyst were firstly pressed followed by sieving to receive particles with diameter ranging from 200 to 315 μm. Typically, 0.2 g of inert quartz sand (200-315 μm in diameter) was thoroughly mixed with 0.1 g of catalyst. Then the solid mixture was packed in the reactor and installed, followed by a leak checking at 40 bar using highly purified N_2 (99.999%). After that, a feed of highly purified CH_4 (99.995 %) of 4.0 mL• min^{-1} and highly purified N_2 (99.999 %) of 4.0 mL• min^{-1} was fed by two mass flow controllers. A flow rate of 1.5 mL• min^{-1} of aqueous H_2O_2 solution (0.12 M) was fed by a HPLC pump. The reaction temperature was 100 °C. The liquid samples were sampled every 0.5 hour and the data of the gas analyzers were noted every

15 minutes. The reaction was performed for 5 hours until the gas analyzer displayed unchanging gas concentrations.

2.4 Product Analysis

The liquid sample was qualitatively analyzed by a mass spectrometer and quantitatively analyzed by high-performance liquid chromatography (HLPC, Agilent 1260 with a column of NUCLEOGEL SUGAR 810 H from Macherey-Nagel). The gas phase was online analyzed by a non-dispersive infrared analyzer (Uras 10E from Hartmann & Braun) and a continuous gas analyzer (EL3020 from ABB).

The methane conversion (X) and selectivity of product i (S_i) are determined in Eq. (1) and Eq. (2):

$$X\,(\%) = \frac{n_{0,CH4} - n_{CH4}}{n_{0,CH4}} \times 100 \quad (1)$$

$$S_i\,(mol\%) = \frac{n_i \times a_i}{\sum_1^i n_i \times a_i} \times 100 \quad (2)$$

Here, $n_{o,CH4}$ represents the initial molar quantity of methane regarding the sampling volume in the inlet of the reactor, and n_{CH4} indicates the molar quantity of methane regarding the sampling volume behind the reactor. n_i is the moles of product i whereas a_i refers to the number of carbon atoms of product i. Turnover frequency (TOF) was defined as moles of liquid phase products per mole of iron and hour (h^{-1}) and volumetric productivity was defined as moles of liquid phase products per reactor volume and second ($mol \bullet ml^{-1}s^{-1}$).

3 Results and discussion

3.1 Characterization

The chemical composition and textual properties of the catalysts are shown in Table 1. In commercial zeolite ZSM-5-C, an impurity of Fe with a content of 175 ppm was detected by the ICP-OES. For the self-synthesized zeolites ZSM-5-S and Si-1, the contents of Fe were below the

detection limit (10 ppm), because ultra-pure precursors of Si and Al were used for the synthesis. For the Fe loaded samples, similar Fe contents of around 0.40 wt. % were obtained except for the Fe(II)/ZSM-5 MDD with a value of 0.62 wt. %. This is because $Fe(acac)_2$ was used as the Fe precursor which is smaller than $Fe(acac)_3$ with regard to the molecular size occupying more positions on the surface of the support which leads to a higher Fe content. Both ZSM-5-S and Si-1 showed higher apparent surface areas (461 m^2/g and 451 m^2/g) and apparent external surface areas (103 m^2/g and 69 m^2/g) than the commercial ZSM-5-C, which possessed values of 383 m^2/g and 30 m^2/g, respectively. For Fe(III)/Si-1 SSIE and Fe(III)/Si-1 MDD, the apparent surface areas dropped to 397 m^2/g and 384 m^2/g with increased apparent external surface areas of 83 m^2/g and 120 m^2/g. The micropore volume dropped to 0.14 cm^3/g and 0.11 cm^3/g. Compared to Fe(III)/Si-1 SSIE, Fe(III)/Si-1 MDD showed much higher increase of apparent external surface area and decrease of micropore volume. As in the MDD method the bulky complex $Fe(acac)_3$ was used as precursor, the probability of loading the Fe species on the external surface is higher, leading to more Fe oxide species distributed at the external surface after calcination, which can block the pores of the zeolite on the surface. For Fe loaded catalysts based on ZSM-5-S, it is interesting that there is no drop of apparent surface area and micropore volume for Fe(II)/ZSM-5 LIE, indicating a high Fe dispersion inside the micropores and less blocking of micropores in this catalyst. Fe(III)/ZSM-5 MDD showed a small decline of apparent surface area and micropore volume to 433 m^2/g and 0.14 cm^3/g, respectively. For Fe(II)/ZSM-5 MDD and Fe(III)/ZSM-5 SSIE, the apparent surface area decreased to 425 m^2/g and 406 m^2/g with both having a little bit lower micropore volume of 0.12 cm^3/g, pointing to partially blocked micropores by large Fe oxide clusters. Notice that, compared to the parent supports, all the catalysts after the introduction of Fe showed significant increase of apparent external surface area, although there can be a contribution of the dispersed iron, this is probably due to the breaking up of the agglomerates in the parent supports during the preparation process. Mild grinding of the parent support of ZSM-5-S by hand in a pestle and mortar confirmed it to be a very loose agglomeration, which is easily broken up (see Table S1).

Table 1 Chemical composition and textural properties of the catalysts.

Sample	Fe (wt. %)	*n*Fe/*n*Al	*n*Fe/*n*Si	S_{BET} [a] (m^2/g)	S_{ex} [b] (m^2/g)	V_p [c] (cm^3/g)
ZSM-5-C	175 ppm	-	-	383	30	0.15

ZSM-5-S	< 10 ppm	-	-	461	103	0.15
Si-1	< 10 ppm	-	-	451	69	0.17
Fe(III)/ZSM-5 SSIE	0.39	0.12	0.0043	406	121	0.12
Fe(III)/Si-1 SSIE	0.40	-	0.0041	397	83	0.14
Fe(III)/ZSM-5 MDD	0.38	0.13	0.0045	433	117	0.14
Fe(II)/ZSM-5 MDD	0.62	0.20	0.0072	425	131	0.12
Fe(III)/Si-1 MDD	0.43	-	0.0047	384	120	0.11
Fe(II)/ZSM-5 LIE	0.39	0.14	0.0045	464	120	0.15

[a] apparent surface area, calculated by BET method. [b] apparent external surface area, calculated by t-plot method. [c] micropore volume, calculated by t-plot method.

Figs. 1a-b show the TEM images of ZSM-5-S and Si-1. For ZSM-5-S, the presence of sub-micrometer crystals (around 175 nm) with a coffin-like morphology could be observed, typical of ZSM-5 crystals. This observation is also consistent with the result of the original synthesis recipe [30]. For Si-1, small particles similar to ellipsoidal with clear edges were obtained. These particles possessed a relative equal size distribution range from 300 nm to 350 nm. These sub-micrometer crystals can help to intensify internal mass/heat transport during reaction.

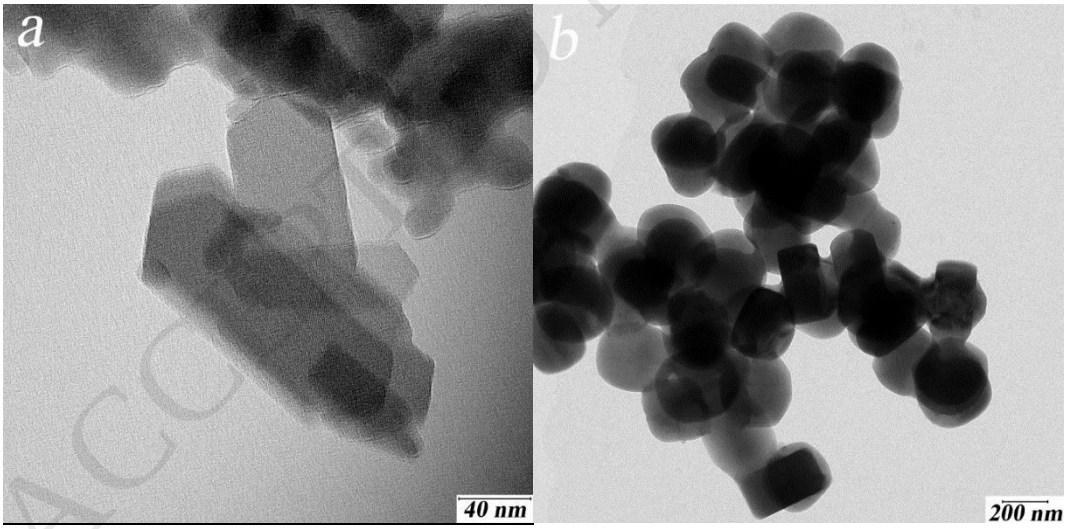

Fig. 1. TEM images of ZSM-5-S (a) and Si-1 (b)

NH_3-TPD profiles of the catalysts are shown in Fig. 2. No acidity could be detected on Si-1 and Fe(III)/Si-1 SSIE. For the parent zeolite ZSM-5-S, two obvious peaks appeared at 212 °C and 423 °C. The peak at 423 °C is assigned to NH_3 strongly adsorbed on Brønsted acid sites [33], while the assignment of the peak at 212 °C is somewhat controversial. It has been attributed to weakly

physisorbed NH_3 coordinated to Lewis acid sites [33] or NH_3 weakly adsorbed on Brønsted acid sites [34, 35]. After the loading of Fe, the temperature of the peak belonging to Brønsted acid sites decreased slightly and in particular, the area of the peak obviously dropped, indicating the Brønsted acid protons in ZSM-5-S were partially replaced by Fe species or the mouths of the micro pores of ZSM-5-S were partially covered by Fe oxide species thus hindering the diffusion of ammonia into the pores. The latter explanation would be consistent with the drop of both the apparent surface area as well as the micropore volume (Table 1) while Fe(II)/ZSM-5 LIE is the only exception.

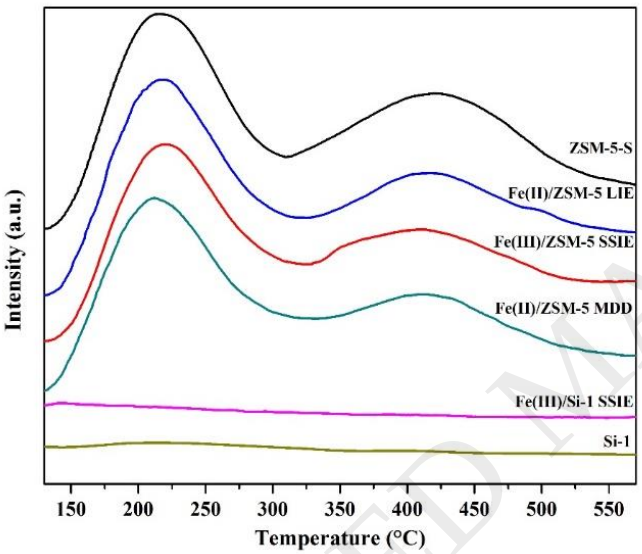

Fig. 2. NH_3-TPD profiles of the catalysts.

H_2-TPR experiments were conducted on all the Fe loaded catalysts, as shown in Fig. 3. The hydrogen consumption for the temperature range of 200-800 °C during the H_2-TPR experiments for the catalysts are summarized in Table 2. Catalysts prepared by different methods showed very different reduction curves. It is clear that all materials feature multiple species of Fe oxide on their surface, although some are more heterogeneous than others. For Fe(III)/Si-1 SSIE, an obvious reduction peak appeared at 495 °C with another high-temperature peak at 665 °C. The H_2/Fe ratio was 1.33 (see Table 2) which was close to 1.5, suggesting that a significant portion of Fe is present as large Fe oxide aggregates which is easily reduced to metallic Fe [23] and not seen in XRD (Fig. S4). Similarly, Fe(II)/ZSM-5 MDD showed an obvious peak at 460 °C with a shoulder peak at 370 °C and a tiny peak at 560 °C with a total H_2/Fe ratio of 1.35, indicating the predominant presence of Fe oxide aggregates (not seen in XRD). In Fe(III)/ZSM-5 SSIE a peak at 475 °C with

two shoulder peaks at 390 °C and 570 °C could be observed. The H_2/Fe ratio was also relative high with the value of 1.21, which also demonstrate a considerable amount of easily reduced iron oxide species but smaller ratio compared to Fe(III)/Si-1 SSIE. A very broad reduction peak could be observed on Fe(III)/ZSM-5 MDD, with the maximum at 400 °C and two shoulder peaks detected at 320 °C and 480 °C, revealing a highly heterogeneous distribution of Fe species. The H_2/Fe ratio was 0.50, which might be attributed to the reduction of a mixture of mononuclear Fe oxide species and α-Fe_2O_3 particles according to I. S. Nam and co-workers [20]. The Fe(III)/Si-1 MDD also showed very broad peaks but appearing at higher temperatures of 555 °C with two shoulder peaks at 405 °C and 635 °C, respectively. A H_2/Fe ratio of 0.65 was detected, which was significantly lower compared to 1.5, this might indicate that most of the Fe species were quite well dispersed and mostly existed as mononuclear Fe oxide species which are very difficult to reduce to metallic Fe. This assumption was consistent with the observation reported in literature for Fe/SiO_2 samples, in which some iron ions have strong interaction with the silica support forming very small iron oxide species that are very stable against reduction to metallic Fe during H_2 reduction [36]. As investigated by J. A. Moulijn and co-workers, the reduction kinetics of iron oxides are also influenced by particle size, morphology, defect density, etc. [37]. Fe(II)/ZSM-5 LIE displayed a tiny and very broad peak with two peaks detected at 405 °C and 505 °C with a very small H_2/Fe ratio value of 0.33. L. J. Lobree et al. studied the oxidation state and the nature of the iron species of Fe dispersed in ZSM-5 catalysts [34]. It was found that three types of Fe^{2+} sites (denoted as type I, II, and III sites) are noticed in Fe/ZSM-5. Types II and III sites, attributed to cationic positions of β and γ, were found to be comparatively resistant to oxidation and reduction. On the other hand, auto-reduction of Fe^{3+} to Fe^{2+} was found during thermal treatment (>523 K) in inert gas or vacuum conditions [34], which was also observed by other authors [38-40]. These factors may cause the silence of partial of the Fe species during the H_2-TPR experiments, leading to a much lower H_2/Fe ratio value and tiny reaction peaks. These observations indicated that a considerable amount of Fe oxide species sensitive to auto-reduction or Fe oxide species located at cationic positions that are difficult to reduce exist in the Fe(II)/ZSM-5 LIE catalyst. The latter is also consistent with the low-temperature N_2 sorption result that reveals a high Fe dispersion inside the micropores and less blocking of micropores in this catalyst.

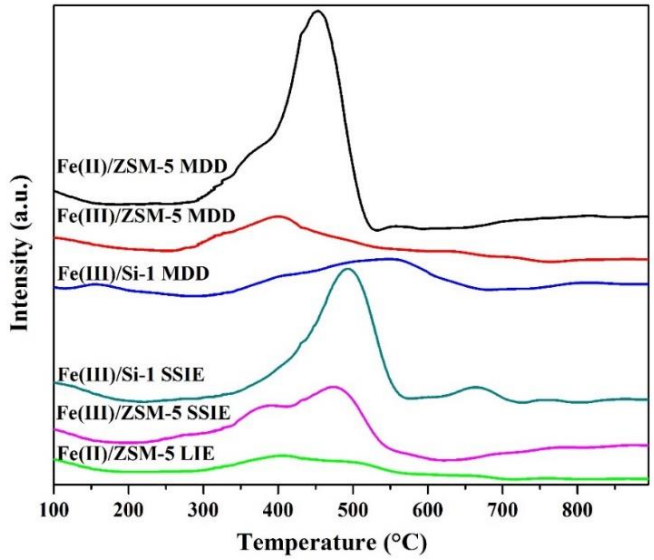

Fig. 3. H_2-TPR profiles of the catalysts.

Table 2 Hydrogen consumption during the H_2-TPR experiments of the temperature range of 200-800 °C for the catalysts investigated in this work.

Sample	*n*Fe/*n*Al	H_2/Fe consumption (mol/mol)
Fe(III)/ZSM-5 SSIE	0.12	1.21
Fe(III)/Si-1 SSIE	-	1.33
Fe(III)/ZSM-5 MDD	0.13	0.50
Fe(II)/ZSM-5 MDD	0.20	1.35
Fe(III)/Si-1 MDD	-	0.65
Fe(II)/ZSM-5 LIE	0.14	0.33

Figs. 4 presents the UV-Vis-DR spectra of the catalysts employed. The spectra differ strongly, indicating a wide distribution of the Fe species present. This may be represented by sub-bands, as shown in the figures and the relative numerical results are shown in Table 3. It was proposed that signals below 300 nm demonstrate isolated Fe species in tetrahedral and octahedral coordinations [19, 41, 42]. Bands range from 300 to 400 nm were attributed to oligomeric Fe oxo entities, whereas signals above 400 nm were attributed to Fe oxide aggregates, revealing probably highly disordered Fe species [19]. However, it was also recently suggested that bands below 300 nm may

appear from binuclear Fe oxo clusters in case of the oxo bridges between the Fe ions are hydroxylated [43].

On the parent zeolites Si-1 and ZSM-5-S, no peak could be obviously detected. For all the Fe loaded catalysts an obvious peak appeared below 300 nm and the relative contribution ranging from 44.8 % to 56.1 % (Table 3), indicating considerable amount of mononuclear Fe oxide species existed in all these samples. For Fe(III)/Si-1 MDD, all the sub-bands were below 400 nm with a dominant sub-band peak present at 235 nm, indicating most Fe existed as isolated Fe species and small oligomeric Fe oxo clusters. This observation is consistent with the H_2-TPR experiment showing a very small and broad reduction peak and a low H_2/Fe ratio value of 0.65, revealing the difficulties of hydrogen reduction of these possibly nano-sized isolated Fe species and oligomeric Fe oxo clusters. According to I. S. Nam and co-workers [20], broad bands appearing between ca. 360 nm and 550 nm for Fe-ZSM-5 are mainly assigned to the d-d transitions of Fe^{3+} ions similar to those for Fe_2O_3. In Fe(III)/Si-1 SSIE, one sub-band appeared around 385 nm which was very close to 400 nm and may be attributed to larger oligomeric Fe species similar to Fe_2O_3. In addition, a sub-band around 515 nm could be found, demonstrating larger Fe oxide aggregates in the sample but not detectable by the XRD (Fig. S4). These large oligomeric Fe species and Fe oxide aggregates would lead to an obvious reduction peak and a large H_2/Fe ratio value, which was confirmed by the H_2-TPR experiments. For Fe(II)/ZSM-5 MDD, sub-bands around 253 nm, 378 nm and 480 nm could be observed. The last one revealed larger Fe oxide aggregates, coinciding with the high H_2/Fe ratio observed in TPR. For Fe(III)/ZSM-5 MDD, sub-bands appeared at around 247 nm, 368 nm and 414 nm. Moreover, there was a comparable larger relative contribution of the larger aggregates (increase in I_3, Table 3). When compared with Fe(II)/ZSM-5 MDD, all peaks shifted to lower wavelengths, which corresponds to Fe species which are more difficult to reduce. This observation was also confirmed by the H_2-TPR curves, that over Fe(II)/ZSM-5 MDD much more obvious reduction peaks could be found and a much larger value of H_2/Fe ratio was obtained compared to Fe(III)/ZSM-5 MDD. Fe(III)/ZSM-5 SSIE and Fe(II)/ZSM-5 LIE showed similar spectra but the sub-bands differed a lot. For Fe(II)/ZSM-5 LIE sub-bands observed at around 255 nm, 367 nm and 432 nm, while for Fe(III)/ZSM-5 SSIE they appeared at 256 nm, 382 nm and 460 nm, i.e. a red shift could be found. Moreover, their relative contribution changed to some extent, creating more I_2 and slightly more I_1 type species at the expense of I_3 species in the Fe(III)/ZSM-5 SSIE. According to A. Brückner and co-workers [44], markedly different redox

behavior of Fe_xO_y clusters and particles exist in Fe-ZSM-5 catalysts and the redox properties of isolated Fe^{3+} sites might change when they coexist with Fe_xO_y clusters in the same sample. Fe_xO_y clusters in Fe(III)/ZSM-5 SSIE may be larger ones mainly located on the surface and covering the mouth of the pores, leading to a significant drop of the apparent surface area and the micro pore volume (Table 1) and more detectable reduction peaks during the H_2-TPR experiments at 475°C. For Fe(II)/ZSM-5 LIE, Fe_xO_y clusters may be much smaller ones mainly located in the pores, especially at cation exchange positions of the ZSM-5-S as no drop of the surface area and the micro pore volume could be found (Table 1). The difference of the Fe_xO_y species in Fe(III)/ZSM-5 SSIE and Fe(II)/ZSM-5 LIE could also be distinguished by their hydrogen reduction properties, which was confirmed by the H_2-TPR experiments. Compared to Fe(II)/ZSM-5 LIE, the reduction peaks could be more obviously observed in Fe(III)/ZSM-5 SSIE with a nearly four times value of consumed H_2/Fe ratio. However, the detailed structure of these different Fe_xO_y species can't be identified in the present work yet.

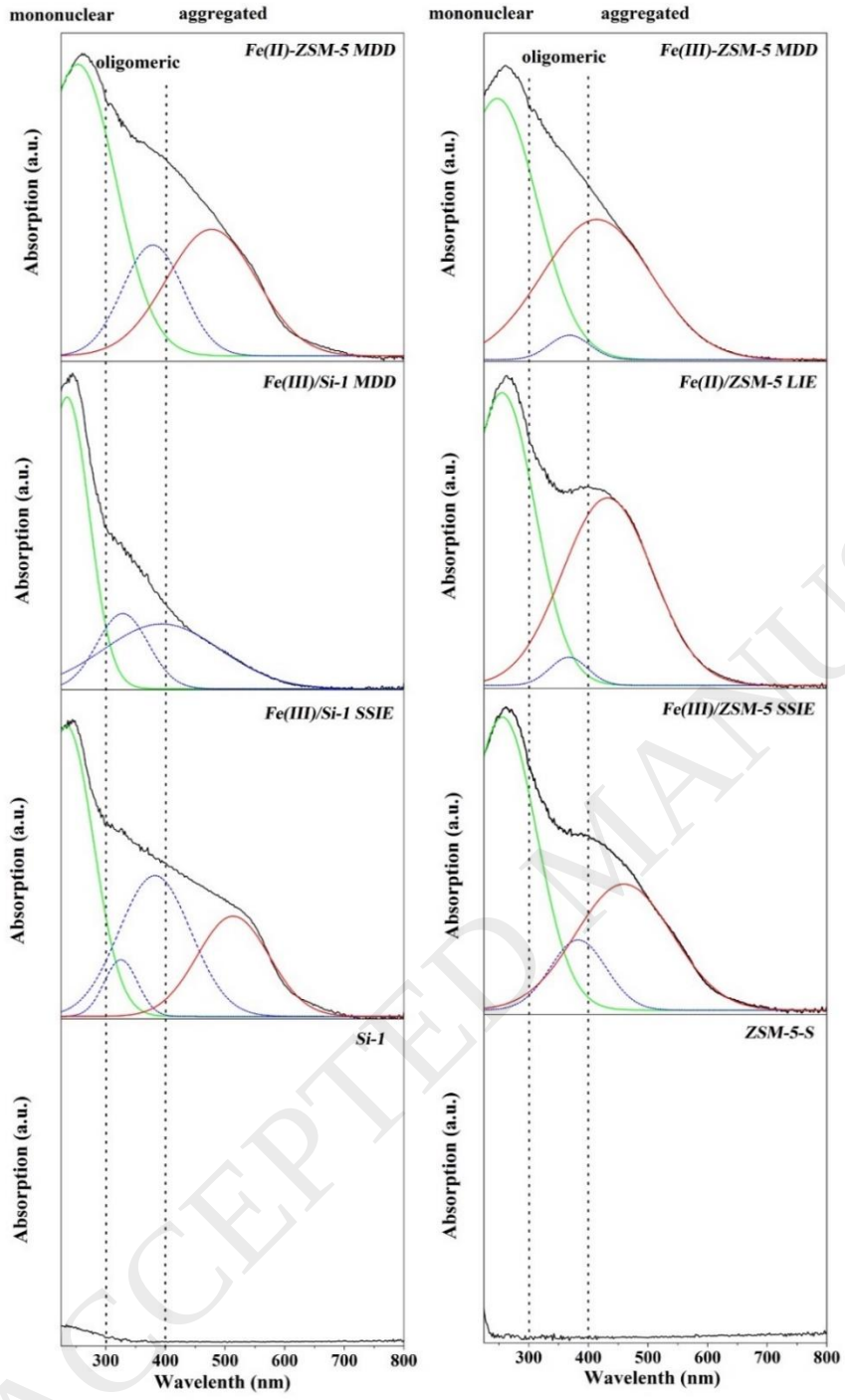

Fig. 4. UV-Vis-DR spectra of the catalysts. Deconvolution of the spectra into sub-bands was performed according to Gauss function to show the relative contribution of these sub-bands.

Table 3 Relative numerical analysis of UV-Vis-DR spectra of Fe based catalysts in Fig. 4. Percentage of the sub-bands deduced from their relative contribution in the different wavelength ranges.

Catalyst	I_1 (%)	I_2 (%)	I_3 (%)
	$\lambda < 300$ nm	$300 < \lambda < 400$ nm	$\lambda > 400$ nm
Fe(II)/ZSM-5 MDD	55.0	16.7	28.3
Fe(III)/ZSM-5 MDD	56.1	2.7	41.2
Fe(III)/Si-1 MDD	53.0	47.0	-
Fe(II)/ZSM-5 LIE	51.7	2.9	45.4
Fe(III)/Si-1 SSIE	44.8	34.5	20.7
Fe(III)/ZSM-5 SSIE	55.5	10.8	33.6

3.2. Catalytic tests

For all the results regarding to the catalytic tests, the gaseous products were mainly CO_2 and O_2 whereas liquid products were formic acid (FA) and formaldehyde (FD) and in some cases methanol (MeOH) with trace amounts less than 0.01 % that was neglected. The only exception with regard to methanol formation was Fe(II)/ZSM-5 LIE with which a methanol selectivity of 3.0 % was measured. Methyl hydroperoxide (CH_3OOH, MHP) was found to be the primary reaction product when relative low temperatures such as 50 °C were chosen for the selective oxidation of methane using H_2O_2 as oxidant [14, 24, 25]. However, when the reaction temperatures increased above 70 °C, no MHP could be detected anymore [14, 45-47]. This may be due to the fact that MHP is not stable at such high temperatures under given conditions. In this work, the reaction temperature was 100 °C and as expected no MHP could be detected.

Table 4 summarizes the catalytic results of different catalysts. For the commercial ZSM-5-C with trace impurity of Fe (Table 1), a considerable methane conversion of 6.5% with a high TOF of 2411 h^{-1} and a very high selectivity of 97.5 % towards FA was obtained. For the synthesized zeolites ZSM-5-S and Si-1 with Fe impurity below 10 ppm (Table 1), no activity could be observed. Also for the two catalysts of Fe(III)/Si-1 SSIE and Fe(III)/Si-1 MDD that are based on silicalite-1, no conversion of methane could be detected, revealing that they do not bear catalytically active Fe sites even though these two catalysts contained considerable content of 0.4 wt.% of Fe (Table 1). Over Fe(III)/ZSM-5 SSIE, a methane conversion of 18.3 % with a FD selectivity of 23.9 % and a FA selectivity of 61.3 % was obtained. The selectivity of CO_2 was 14.8 %, indicating a high level of over-oxidation of methane. The TOF and volumetric productivity were 255 h^{-1} and $2.7\times10^{-}$

^{6} mol•ml^{-1}s^{-1}, respectively. A H_2O_2 conversion of 88.5 % with a H_2O_2 utilization of 32.1 % was reached. When comparing the catalysts prepared with the MDD method, the methane conversion increased from 18.1 % with Fe(III)/ZSM-5 MDD to 19.1 % with Fe(II)/ZSM-5 MDD. Similar FD selectivities (19.7 % for Fe(III)/ZSM-5 MDD and 19.1 % for Fe(II)/ZSM-5 MDD) were obtained. The selectivity of CO_2 dropped significantly from 15.6 % to 9.5 %, pointing out that the over-oxidation could be retarded to some extent with Fe(II)/ZSM-5 MDD. A lower TOF value of 190 h^{-1} was found compared to that of 287 h^{-1} over Fe(III)/ZSM-5 MDD, this may due to a much higher Fe content of Fe(II)/ZSM-5 MDD (see Table 1). It was interesting that a higher volumetric productivity of 3.2×10^{-6} mol•ml^{-1}s^{-1} and a higher value of H_2O_2 utilization of 46.8 % together with a lower H_2O_2 conversion of 74.3 % was obtained over Fe(II)/ZSM-5 MDD. For Fe(II)/ZSM-5 LIE, the methane conversion considerably increased to 23.5 % with a FD selectivity of 22.6 % and a FA selectivity of 64.4 %. Little amount of methanol was also detected with a selectivity of 3.0 %. The selectivity of CO_2 was 9.9 %, indicating a relative low level of over-oxidation. Compared to other Fe loaded catalysts, the highest TOF of 303 h^{-1} together with a relative high volumetric productivity of 3.1×10^{-6} mol•ml^{-1}s^{-1} was received. The H_2O_2 conversion and utilization were 95.2 % and 34.5 %, respectively.

According to G. J. Hutchings and co-workers [14], with Cu-Fe/ZSM-5 as catalysts a TOF of 0.3 h^{-1}, a volumetric productivity of 9.4×10^{-9} mol•ml^{-1}s^{-1} and a H_2O_2 utilization of 3.5 % were obtained at the highest methane conversion of 0.5 % in a fixed-bed reactor. As it can be seen from Table 4, when the selective oxidation of methane was conducted over sub-micrometer sized crystals of Fe/ZSM-5 catalysts (with a similar Fe content to the reference (0.4 wt. %)) in a micro fixed-bed reactor to enhance internal and external mass transport of the overall reaction, the TOFs and volumetric productivities could be promoted more than two orders of magnitude with around ten times higher H_2O_2 utilization. Similar significant promotion of TOFs and volumetric productivities was also observed in our former work [27]. A considerable methane conversion with very high TOF, FA selectivity and efficient H_2O_2 utilization could be observed over HZSM-5 with trace amount (175 ppm) Fe impurity. Over HZSM-5 with Fe below 10 ppm as ultra-pure precursors were used on purpose for the synthesis, no activity could be found, indicating that Brønsted acid sites can't activate methane alone. Catalysts based on silicalite-1 with similar Fe content showed no activity, demonstrating that acidity plays a critical role in obtaining special structure of Fe species as the active sites or acidity serves as an important promoter for the reaction. Different

Fe/ZSM-5 catalysts based on the different preparation methods for the post-synthetic Fe loading on ZSM-5 showed similar methane activation activities and similar methane conversion from 18.1 % to 23.5 % (Table 4), indicating a low sensitivity of these investigated preparation methods towards catalytic activities under given conditions. However, the selectivity was different when Fe(II) was used as the precursor. The calcined catalysts showed a better performance for retarding of over-oxidation, as the selectivity of CO_2 was below 10 % over Fe(II)/ZSM-5 MDD and Fe(II)/ZSM-5 LIE. Furthermore, Fe(II)/ZSM-5 MDD showed the lowest H_2O_2 conversion and the highest H_2O_2 utilization of the prepared catalysts.

Notice that, over the commercial HZSM-5 with a trace amount of Fe impurity of 175 ppm, a considerable methane conversion of 6.5 % was received under given conditions. Thus, to obtain a methane conversion around 20 %, only threefold amount of Fe is necessary, i.e. a Fe content of about 0.05 wt. %. This means that only about 10 % of the introduced Fe species in the catalysts play an important role during the reaction while most of introduced Fe species are silent. If one considers that not all of the 175 ppm Fe are active sites, one can imagine that it is a really tiny amount of active sites being highly active. On the other hand, the characterization of ZSM-5 based post-synthesis catalysts revealed interesting differences and the catalytic results showed high levels of TOF, volumetric productivity and H_2O_2 utilization. However, the correlation between these differences and catalytic performance of the catalysts is not clear, which could be caused by the relatively small part of the Fe species that are expected to play an important role or indicates that the reaction may not be driven by simple active sites but could be the interaction of different types of iron species and/or the acid sites. Thus, further fundamental research to unravel the generation mechanism of the active sites and these interactions remains very important to be able to design an optimal catalyst and process.

Table 4 Catalytic results of different catalysts.

Catalyst	CH_4 conversion %	Selectivity %				TOF h^{-1}	Volumetric productivity $mol \cdot ml^{-1}s^{-1}$	H_2O_2 conversion %	H_2O_2 utilization [a] %
		MeOH	FD	FA	CO_2				
ZSM-5-C	6.5	0	0	97.5	2.5	2411	1.1×10^{-6}	25.3	55.3
ZSM-5-S	0.1	0	0	0	0	0	0	1.7	0
Si-1	0.1	0	0	0	0	0	0	2.0	0
Fe(III)/ZSM-5 SSIE	18.3	0	23.9	61.3	14.8	255	2.7×10^{-6}	88.5	32.1
Fe(III)/Si-1 SSIE	0.0	0	0	0	0	0	0	4.3	0
Fe(III)/ZSM-5 MDD	18.1	0	19.7	64.7	15.6	287	3.0×10^{-6}	86.8	37.2
Fe(II)/ZSM-5 MDD	19.1	0	19.1	71.4	9.5	190	3.2×10^{-6}	74.3	46.8
Fe(III)/Si-1 MDD	0.2	0	0	0	0	0	0	21.2	0
Fe(II)/ZSM-5 LIE	23.5	3.0	22.6	64.4	9.9	303	3.1×10^{-6}	95.2	34.5

[a] H_2O_2 utilization: the percentage of O_2 incorporation from decomposed H_2O_2 into liquid products.

4. Conclusions

Sub-micrometer sized crystals of HZSM-5 and silicalite-1 with Fe impurities below 10 ppm were successfully synthesized. Different methods and different Fe precursors were used for post-synthetic loading of 0.40 wt. % Fe of Fe/ZSM-5 zeolites. All the catalysts were applied for the selective oxidation of methane with aqueous H_2O_2, conducted in a micro fixed-bed reactor to enhance the mass transport. Compared to literature, the TOFs and volumetric productivities could be more than two orders of magnitude enhanced and around ten times higher H_2O_2 utilization could be obtained. ZSM-5 with trace amount (175 ppm) of Fe impurity, which is typical when using standard precursors for the synthesis, already showed considerable methane activation ability. On ZSM-5 with Fe content below 10 ppm as ultra-pure precursors were used on purpose for the synthesis, no activity was found, revealing that Brønsted acid sites can't activate methane alone under given conditions and it is important to obtain Fe free ZSM-5 samples as basis for the study of methane oxidation with iron based catalysts. Fe loaded on the same structure of silicalite-1 showed no activity, even bearing the same Fe content. Different Fe/ZSM-5 catalysts based on

different preparation methods showed similar methane activation activities, indicating a low sensitivity of these post-synthesis methods under given conditions when sub-micrometer sized crystals of HZSM-5 were used as the support. Catalysts based on Fe(II) as the precursor showed a better performance for the retarding of over-oxidation. The liquid ion exchange method with Fe(II) resulted in the only catalyst, which produced methanol.

Acknowledgments

The authors thank ENMIX for offering us a wonderful collaborative environment. H. Zuo acknowledges the financial support from CSC. V. Meynen thanks the FWO Flanders for the mobility grant (V4.031.16N). We thank Robin Himmelmann for the support of H_2-TPR experiments. Thanks also go to Karen Leyssens for the UV-Vis-DR measurements and Paul Rößner & Fabian Guba for the TEM measurements.

References:

[1] Z. Guo, B. Liu, Q. Zhang, W. Deng, Y. Wang, Y. Yang, Chem. Soc. Rev. 43 (2014) 3480-3524.

[2] A.I. Olivos-Suarez, À. Szécsényi, E.J.M. Hensen, J. Ruiz-Martinez, E.A. Pidko, J. Gascon, ACS Catal. 6 (2016) 2965-2981.

[3] N. Dietl, M. Schlangen, H. Schwarz, Angew. Chem., Int. Ed. 51 (2012) 5544-5555.

[4] A. Holmen, Catal. Today 142 (2009) 2-8.

[5] J.S. Woertink, P.J. Smeets, M.H. Groothaert, M.A. Vance, B.F. Sels, R.A. Schoonheydt, E.I. Solomon, Proc. Natl. Acad. Sci. U. S. A. 106 (2009) 18908-18913.

[6] T.V. Choudhary, V.R. Choudhary, Angew. Chem., Int. Ed. 47 (2008) 1828-1847.

[7] N.D. Spencer, J. Catal. 109 (1988) 187-197

[8] A.E. Shilov, G.B. Shul'Pin, Chem Rev. 97 (1997) 2879-2932.

[9] R.A. Periana, D.J. Taube, S. Gamble, H. Taube, T. Satoh, H. Fujii, Science. 280 (1998) 560-564.

[10] E.M. Alayon, M. Nachtegaal, M. Ranocchiari, J.A. van Bokhoven, Chem. Commun. 48 (2012) 404-406.

[11] V.I. Sobolev, K.A. Dubkov, O.V. Panna, G.I. Panov, Catal Today. 24 (1995) 251-252.

[12] V. Fornes, C. Lopez, H.H. Lopez, A. Martinez, Appl Catal A-Gen. 249 (2003) 345-354.

[13] R. Palkovits, M. Antonietti, P. Kuhn, A. Thomas, F. Schüth, Angew. Chem., Int. Ed. 48 (2009) 6909-6912.

[14] J. Xu, R.D. Armstrong, G. Shaw, N.F. Dummer, S.J. Freakley, S.H. Taylor, G.J. Hutchings, Catal. Today 270 (2016) 93-100.

[15] S. Grundner, M.A.C. Markovits, G. Li, M. Tromp, E.A. Pidko, E.J.M. Hensen, A. Jentys, M. Sanchez-Sanchez, J.A. Lercher, Nat. Commun. 6 (2015) 7546-7554.

[16] R.S. Hanson, T.E. Hanson, Microbiol. Rev. 60 (1996) 439-471.

[17] H. Dalton, Philos. Trans. R. Soc., B 360 (2005) 1207-1222.

[18] R. Balasubramanian, S.M. Smith, S. Rawat, L.A. Yatsunyk, T.L. Stemmler, A.C. Rosenzweig, Nature 465 (2010) 115-119.

[19] M. Schwidder, S. Heikens, A. Detoni, S. Geisler, M. Berndt, A. Bruckner, W. Grunert, J. Catal. 259 (2008) 96-103.

[20] J. Park, J. Choung, I. Nam, S. Ham, Appl. Catal., B 78 (2008) 342-354.

[21] H. Chen, W.M.H. Sachtler, Catal. Today 42 (1998) 73-83.

[22] A. Guzmán-Vargas, G. Delahay, B. Coq, E. Lima, P. Bosch, J. Jumas, Catal. Today 107-108 (2005) 94-99.

[23] M. Schwidder, M. Kumar, K. Klementiev, M. Pohl, A. Bruckner, W. Grunert, J. Catal. 231 (2005) 314-330.

[24] C. Hammond, M.M. Forde, M.H. Ab Rahim, A. Thetford, Q. He, R.L. Jenkins, N. Dimitratos, J.A. Lopez-Sanchez, N.F. Dummer, D.M. Murphy, A.F. Carley, S.H. Taylor, D.J. Willock, E.E. Stangland, J. Kang, H. Hagen, C.J. Kiely, G.J. Hutchings, Angew. Chem., Int. Ed. 51 (2012) 5129-5223.

[25] C. Kalamaras, D. Palomas, R. Bos, A. Horton, M. Crimmin, K. Hellgardt, Catal. Lett. 146 (2016) 483-492.

[26] A.J. Vanhengstum, J.G. Vanommen, H. Bosch, P.J. Gellings, Appl. Catal. 5 (1983) 207-217.

[27] M.G. White, Catal. Today 18 (1993) 73-109.

[28] A. Hanu, S. Liu, V. Meynen, P. Cool, E. Popovici, E.F. Vansant, Microporous Mesoporous Mater. 95 (2006) 31-38.

[29] H. Zuo, V. Meynen, E. Klemm, Chem. Ing. Tech. 89 (2017) 1759-1765.

[30] R. Van Grieken, J.L. Sotelo, J.M. Menéndez, J.A. Melero, Microporous Mesoporous Mater. 39 (2000) 135-147.

[31] A.E. Persson, B.J. Schoeman, J. Sterte, J.E. Otterstedt, Zeolites 14 (1994) 557-567.

[32] A. Shishkin, P. Carlsson, H. Härelind, M. Skoglundh, Top. Catal. 56 (2013) 567-575.

[33] S. Brandenberger, O. Kroecher, A. Wokaun, A. Tissler, R. Althoff, J. Catal. 268 (2009) 297-306.

[34] L.J. Lobree, I. Hwang, J.A. Reimer, A.T. Bell, J. Catal. 186 (1999) 242-253.

[35] B. Hunger, J. Hoffmann, O. Heitzsch, M. Hunger, J. Therm. Anal. 36 (1990) 1379-1391.

[36] S. Yuen, Y. Chen, J.E. Kubsh, J.A. Dumesic, N. Topsoe, H. Topsoe, J. Phys. Chem. C 86 (1982) 3022-3032.

[37] O.J. Wimmers, P. Arnoldy, J.A. Moulijn, J. Phys. Chem. 90 (1986) 1331-1337.

[38] R. Joyner, M. Stockenhuber, J. Phys. Chem. B 103 (1999) 5963-5976.

[39] J. Pérez-Ramírez, G. Mul, F. Kapteijn, J.A. Moulijn, A.R. Overweg, A. Doménech, A. Ribera, I.W.C.E. Arends, J. Catal. 207 (2002) 113-126.

[40] P. Fejes, J.B. Nagy, K. Lazar, J. Halasz, Appl Catal A-Gen. 190 (2000) 117-135.

[41] M.S. Kumar, M. Schwidder, W. Grunert, A. Bruckner, J. Catal. 227 (2004) 384-397.

[42] S. Bordiga, R. Buzzoni, F. Geobaldo, C. Lamberti, E. Giamello, A. Zecchina, G. Leofanti, G. Petrini, G. Tozzola, G. Vlaic, J. Catal. 158 (1996) 486-501.

[43] G.D. Pirngruber, P.K. Roy, R. Prins, Phys. Chem. Chem. Phys. 8 (2006) 3939-3950.

[44] M. Santhoshkumar, M. Schwidder, W. Grunert, U. Bentrup, A. Bruckner, J. Catal. 239 (2006) 173-186.

[45] G.V. Nizova, G. Suss-Fink, G.B. Shulpin, Chem. Commun. (1997) 397-398.

[46] A.K.M.L. Rahman, M. Kumashiro, T. Ishihara, Catal. Commun. 12 (2011) 1198-1200.

[47] J. Min, H. Ishige, M. Misono, N. Mizuno, J. Catal.198 (2001) 116-121.